Sl. No.	IIT Ropar List of Recent Publications with Abstract Coverage: May, 2024
A	**Book(s)**
1.	Modern materials and manufacturing techniques **R Kant** - Book, ISBN: 9781003852223, CRC Press, 2024 **Abstract:** The text provides the reader with an in-depth understanding of the need for next-generation materials and manufacturing, especially in terms of their designing process, manufacturing, upscaling, and finally their selection for industrial applications. It further discusses path-planning strategies for robot-based additive manufacturing. Discusses synthesis, modelling, and analysis of green composites and functionally graded materials. Explains hybrid manufacturing processes to address the challenges faced by the manufacturing industries. Covers additive manufacturing of advanced materials for smart products. Presents applications of lasers for sensing, characterization, and material processing. Illustrates principles and applications of 4D printing and cold spray-based additive manufacturing. The book focuses on sustainability in material and manufacturing processes. It covers important topics such as material recycling, optimal utilization of resources, green materials, improving surface inhomogeneity, stable material properties, and utilization of renewable energy sources. The text highlights the applications of deep learning for diagnosis and analysis in materials and manufacturing technologies. It is primarily written for senior undergraduate, graduate students, and academic researchers in the fields of manufacturing engineering, industrial and production engineering, materials science and engineering, and mechanical engineering.
2.	Postcolonial Indian city-literature: Policy, politics and evolution **D Ray** - Book, ISBN: 9781003166337, Routledge, 2022 **Abstract:** How is the city represented through literature from the post-colonies? This book searches for an answer to this question, by keeping its focus on India—from after Independence to the millennia. How does the urban space and the literature depicting it form a dialogue within? How have Indian cities grown in the past six decades, as well as the literature focused on it? How does the city-lit depart from organic realism to dissonant themes of “reclamation”? Most importantly—who does the city (and its narratives) belong to? Through the juxtaposition of critical theories, sociological data, urban studies and variant literary works by a wide range of Indian authors, this book is divided into four temporal phases: the nation-building of the 50–60s, the dictatorial 70s, the neoliberalization of the 80–90s and the early 2000s. Each section covers the dominant socio-political thematics of the time and its effect on urbanism along with historical data from various resources, followed by an analysis of contemporaneously significant literary works—novel, short stories, plays, poetry and graphic novel. Each chapter comments on how literature, perceived as a historical phenomenon, frames real and imagined constructs and experiences of cities. To give the reader a more expansive idea of the complex nature of city-lit, the literary examples abound not only “Indian Writings in English,” but vernacular, cult-works as well with suitable translations. With its focus on philosophy, urban studies and a unique canon of literature, this book offers elements of critical discussion to researchers, emergent university disciplines and curious readers alike.
B	**Book Chapter(s)**
3.	Advances in the solar thermal systems assisted production of green hydrogen: its analysis, scaling-up techniques, and economics aspects as applied to tropical regions J Patel, AR Patel**, H Tyagi** - Challenges and Opportunities in Green Hydrogen Production: Book

	Chapter, 2024 **Abstract:** Hydrogen (H2) production currently faces difficulties with regard to its feasibility in terms of cost competitiveness when compared to traditional fossil fuel-based H2 production systems. In these conditions, producing green hydrogen (GH) using solar thermal systems (STS) is undoubtedly a viable and promising option. The present study examines recent developments in the application of various STSs for the production of GH with a focus on their actual analytical approach, application, scaling-up strategies, and economic viability, particularly in the context of tropical regions. GH offers an opportunity to decarbonize various critical sectors, such as transportation, industry, and power generation. It facilitates a smooth transition to a low-carbon economy and aids nations in achieving their climate goals. The chapter opens up with an emphasis on the value of renewable energy sources for the generation of power for any country in the introductory part. An overview of the various STSs used to produce H2 is provided in the section that follows. The effectiveness and practicality of the new STSs used for GH generation are also critically assessed. This comprises life cycle evaluations, techno-economic analysis, and modeling and simulation approaches. Finally, the economics of GH production in developing nations using STSs is investigated. The critical observation and findings are intended to educate policymakers, researchers, and industry stakeholders on the potential of these technologies to promote sustainable development and energy transition in the targeted tropical regions.
4.	Challenges with sustainable green hydrogen production: Role of materials, design, multi-scale modeling, and up-scaling **T Rohilla, M Kumar** - Challenges and Opportunities in Green Hydrogen Production: Book Chapter, 2024 **Abstract:** In recent years, green hydrogen has emerged as the prime solution for meeting the challenges of the energy crisis and climate change posed by the overuse of fossil fuels. Green hydrogen is the hydrogen produced from water-splitting reactions driven by renewable and sustainable energy resources such as solar, geothermal, hydro, wind, and biomass resources that do not emit greenhouse gases, such as carbon dioxide and others. There are other different mechanisms and conversion routes for producing green hydrogen. Due to the increasing demand for hydrogen for various applications such as steel, off-grid electricity, ammonia, agriculture, and automobiles, there is a need for large-scale green hydrogen production. This technology enhancement is required to meet the coveted target of USD 1 per kg, . There are some established technologies such as alkaline, polymer electrolyte membranes, and solid-oxide electrolyzers for hydrogen production. However, several challenges in their efficient utilization are being addressed through the use of suitable materials and design modifications at the appropriate scale of production. Therefore, there is a requirement for a multiscale modeling framework for the selection of compatible and efficient material, and optimum design parameters keeping in mind the safety aspects and the economic viability of scaling criteria. Modeling and digital-twin development are high-performance tools that enhance and utilize the capability of electrolyzers and the associated balance of plants to develop efficient coupling with renewable resources for more efficient hydrogen production. This chapter focuses on the modeling tools and techniques that have been employed to develop reliable models and digital twins of electrolyzers for understanding optimum operating conditions to produce cost-effective hydrogen with high efficiency of conversion in the optimum pressure range. In addition to this, challenges with materials and design aspects have been discussed with a focus on the development of efficient, low-cost electrocatalysts for anode and cathode, porous transport layers, gas diffusion layers, separators, and electrolyte membranes to achieve high conversion efficiency, low gas crossover, and others. In addition, in this chapter, a discussion of the different cell architectures and modular designs of membrane electrolyzers is presented to achieve better conversion efficiency, low gas dissolution, and higher flow rate of the produced hydrogen with minimum components. Moreover, scaling or sizing of the green hydrogen production systems from cells and stacks up to

	plants (10 MW to 1 GW) requires thorough techno-economic analysis taking into account the renewable energy capacity of the region and the costs of the equipment. Thus, discussions on the techno-economic analyses and case studies of such region-based and renewable energy resource-specific hydrogen production have been presented.
5.	CO2 transportation facilities: Economic optimization using genetic algorithm F Hourfar**, MM Laljee**, A Ahmadian… - Carbon Capture, Utilization, and Storage Technologies: Book Chapter, 2024 **Abstract:** According to recent studies, it has been proven that reducing greenhouse gas (GHG) emissions is imperative to prevent global warming and protect the environment [1, 2]. One of the viable options of GHG reduction is carbon capture and storage (CCS) technologies [3] in which CO2 is captured from different sources (such as power plants), then it is transported through pipelines [4, 5], and finally it is being sequestrated for long term in appropriate onshore/offshore reservoirs to prevent entering the atmosphere, which results in reducing adverse greenhouse gas impacts. In recent decades, despite the advancement of carbon capture technology to the point of commercial deployment and acknowledgement of underground reservoir storage as a secure solution, CO2 transportation systems are still a challenging issue [6]. The most expensive components of a CCS chain are the CO2 capture technologies [7]. However, optimal CO2 transportation facility design can drastically lower the project's overall cost [8–11], especially when the source-sink distance is greater than 100 km. Recent studies demonstrate that the cost of transport facilities in a CCS project is more than anticipated [12]. Therefore, they must be designed in an economically optical manner. Moreover, a cost model intertwined with the pipeline's hydrodynamic model is necessary [13].
6.	Energy Policy: Formulation, monitoring, and adaptation for moving towards a low carbon economy **AR Patel, P Sarkar, H Singh, H Tyagi** - The Costs of Climate Change Mitigation Innovations: Book Chapter, 2024 **Abstract:** It is essential to understand the connection between energy production, greenhouse gas emissions, and global warming. A worldwide sustainability plan has unified several nations under one roof. The paper offers a comprehensive methodology and factors to be taken into account when developing a sustainable energy policy for a country. When assessing the effectiveness of various nations' efforts to adapt to the production, usage, and consequences of energy sources, the energy trilemma index is frequently used. Nations have varied policies and strategies for reaching sustainable energy goals due to variances in their resources, liabilities, geographic position, stage of development, fuel resources, energy demand, populations, economic growth, and other considerations. There are more and more signs that countries are starting to converge towards a common policy strategy, but there are still a lot of areas that may need improvement. The paper also highlights some important grey areas, including how nuclear and hydro energy are handled, how energy and emissions are accounted for in policy, how emissions are controlled in the transportation sector, how legal provisions for renewable energy are proposed, social responsibilities, energy certificates, embodied energy and emission data, etc. These elements demand that researchers and decision-makers examine this issue from a comprehensive angle. Given this, it is crucial to develop an international, cross-border energy plan that takes into account how the economy and environment affect energy production.
7.	Permafrost-induced hazard zonation using satellite data-driven multi-parametric approach employing AHP techniques in Alaknanda Valley, Uttarakhand, India T Ghosh, AC Pandey, BR Parida…**RK Tiwari** - Geo-information for Disaster Monitoring and Management: Book Chapter, 2024 **Abstract:** Permafrost is one of the key components of the mountain cryosphere. An increase in

	global air temperature is leading to the melting of permafrost. Degradation and thawing of permafrost may induce multiple effects on the landscape, such as ground subsidence, increased frequency of landslides and rock falls due to destabilization of permafrost-covered slopes, further harming the infrastructures like roads, bridges, dams, buildings, etc. Climate models can predict further degradation of permafrost in the high mountain regions due to an increase in air temperature, resulting in changes in the terrestrial ecosystem and frequent permafrost-induced hazards. In the past decade, the area under investigation has experienced multiple natural hazards like slope failures, landslides, rock-ice avalanches, etc. In this study, assessment and hazard zonation of geohazards associated with mountain permafrost was attempted using AHP (Analytical Hierarchical Process) based multi-parametric approach. Based on its hazard susceptibility, the study area was categorized into three zones, namely, low, moderate, and high. Their corresponding area were 1738.28 km^2, 8945.77 km^2, and 518.89 km^2, respectively. The model output provided probable areas of hazard occurrence based on select topographical and climatic factors. Identifying regions with high hazard potential will help better understand the spatial distribution of such potentially hazardous sites within the study area, resulting in better mitigation and disaster management capabilities.
8.	Superhydrophobic coatings: Insights and real-world applications S Keshri, S Sudha, S Roychowdhury, **K Kumar** - Functional Coatings: Innovations and Challenges: Book Chapter, 2024 **Abstract:** Mother Earth inspires scientists and researchers worldwide every day to unveil its mysteries. We can imitate biology to create nanomaterials, nanodevices, and processes that have desirable qualities thanks to the recently developed discipline of biomimetics. Applications in both research and industry have shown a unique interest in biomimetic surfaces with specific wettability and adaptability. Thanks to nanotechnology, surface chemistry, and architecture, improvements have made superhydrophobicity a practical goal. Superhydrophobic surfaces are distinctive due to several notable developments, and they are predicted to continue to advance for many years. This chapter will focus on the most up-to-date developments in the physical characterization of numerical modeling, experimental methods, and practical uses of superhydrophobic surfaces. Superhydrophobic coatings, which are mechanically stable, thermally inert, and chemically inert, have vast promise in every area of human life. The biological, culinary, and aerospace industries could all benefit significantly from using superhydrophobic materials. References
9.	Two-dimensional nanomaterial-based polymer nanocomposites for rechargeable lithium-ion batteries J Jyoti, **M Sandhu**, BP Singh, SK Tripathi - Two‐Dimensional Nanomaterials-Based Polymer Nanocomposites: Processing, Properties and Applications: Book Chapter, 2024 **Abstract**: The growing demand for portable devices and electric vehicles (EVs) resulted in rechargeable lithium-ion batteries (LIBs) gaining significant attention in research because of their excellent properties, such as high energy density, high capacity, and high voltage. Over the past few decades, the electrochemical properties and efficiency of LIBs have been enhanced, but several issues remain such as thermal management, the high cost of lithium, moderate storage capacity, and low diffusion rate, which prevent the use of its full potential. With an increasing demand for rechargeable batteries, researchers are continuously developing various fillers that fulfill the basic requirement of flexibility and high-power/energy density materials. Two-dimensional materials (MXene, graphene, black phosphorus, transition metal oxide, etc.) are being significantly used in energy conversion and storage devices (ECSD). These materials are showing excellent potential for energy storage (ES) applications because of their large specific surface area (SSA), efficient ion transportation between the layers, improved ion adsorption, and fast surface redox reactions. The electrode material with high rate and outstanding cyclic stability

	features has been widely used for the development of ES applications. The main emphasis in this chapter is on the recent advancement, future development, and scientific task of various innovative 2D polymer nanocomposites for the fabrication of cathode and anode electrodes that are used in LIBs. Finally, future prospects and critical challenges of 2D materials are also addressed.
C	**Conference Proceeding(s)**
10.	A double cross-coupled delay cell for high-frequency differential ring VCOs **MK Singh, MK Gautam, P Singh,** R Nagulapalli, **DM Das, M Sakare** - 2023 IEEE Asia Pacific Conference on Circuits and Systems (APCCAS), 2024 **Abstract:** This paper presents a double cross-coupled delay cell (DCC-Delay cell) incorporated in a two-stage ring voltage-controlled oscillator (RVCO) that enhances its operating frequency. The DCC-Delay cell employs two cross-coupled transistor pairs, one in a pull-up network and the other in a pull-down network. This design configuration effectively reduces the time required for discharging the output node, allowing for higher operating frequencies. The RVCO's frequency is controlled by a PMOS transistor-based capacitance between the two output nodes. Simulations were performed in 65 nm CMOS technology after post-layout parasitic extraction using a 1 V supply voltage. The phase noise of DCC-Delay cell-based RVCO is -103.4 dBc/Hz at an offset frequency of 1 MHz, operating at 1.2 GHz while dissipating 6.2mW power. The DCC-Delay cell-based RVCO achieves a 55% improvement in operating frequency compared to conventional RVCO while experiencing only slightly increasing power dissipation. The figure of merit (FOM) of the DCC-Delay cell-based RVCO is -157 dBc/Hz at a 1 MHz offset frequency, rivaling other RVCO architectures in the existing literature.
11.	A framework for performance optimization of internet of things applications O Almurshed… **AK Kaushal**…**N Auluck**… - 2023 International Workshop held at the 29th International Conference on Parallel and Distributed Computing, 2024 **Abstract:** A framework to support optimised application placement across the cloud-edge continuum is described, making use of the Optimized-Greedy Nominator Heuristic (EO-GNH). The framework can be employed across a range of different Internet of Things (IoT) applications, such as smart agriculture and healthcare. The framework uses asynchronous MapReduce and parallel meta-heuristics to support the management of IoT applications, focusing on metrics such as execution performance, resource utilization and system resilience. We evaluate EO-GNH using service quality achieved through real-time resource management, across multiple application domains. Performance analysis and optimisation of EO-GNH has also been carried out to demonstrate how it can be configured for use across different IoT usage contexts.
12.	Control of five leg inverter based two motor drive under current sensor failure A Azeem, **AVR Teja, S Payami** - 2023 IEEE International Conference on Power Electronics, Smart Grid, and Renewable Energy (PESGRE), 2024 **Abstract:** This paper proposes a current sensor fault tolerant (CSFTC) control of the five-leg inverter (FLI) that drives the two induction motors independently. The simulation test validation is carried out when all current sensors or power supplies used for current sensor undergo failure. The proposed solution suggests employing generalized equations that leverage the PWM-generated voltage and the angular speed of the rotor. These equations enable the reconstruction of the stator phase current in the stationary reference frame (α-β).This scheme minimizing the system dependency on sensors in noisy environment. The proposed scheme is verified at different operating states of the drive system through the MATLAB/Simulink platform. The simulation result validate the effectiveness and feasibility of proposed scheme.
13.	Improved resistive switching and synaptic characteristics on 2-D graphene/MoS2/graphene

	memristor using O2 plasma irradiation **K Varshney, P Shukla**, B Prakash, **DM Das, B Rawat** - 8th IEEE Electron Devices Technology and Manufacturing Conference (EDTM), 2024 **Abstract:** Two-dimensional MoS 2 -based memristors have demonstrated remarkable performance attributes, such as precise conductance control and robust operation. However, their limited ON/OFF conductance ratio has posed challenges in terms of reading accuracy and energy efficiency. In addressing this issue, we propose a novel approach involving oxygen plasma irradiation of chemical vapor-deposited trilayer MoS 2 memristors. The proposed memristor exhibits a significantly higher ON/OFF current ratio of approximately (10 2), lower OFF-state current (3μA), the capability for multilevel states, and linear and symmetric conductance changes within the nominal device structure. These improvements stem from the substantial increase in the conductive path due to the presence of MoO 3 defect states. The enhanced switching characteristics position oxygen-irradiated MoS 2 devices as promising candidates for large-scale crossbar array applications.
14.	UWB circular metal mesh transparent antenna U Rafique, SM Abbas, **S Agarwal**… - 18th European Conference on Antennas and Propagation (EuCAP), 2024 **Abstract:** his paper presents the design of a novel co-planar waveguide (CPW)-fed circular metal mesh (MM) transparent antenna (TA) for ultra-wideband (UWB) applications. To achieve transparency, the MM technique is utilized on both the conductor and the dielectric substrate. To achieve broadband impedance matching in the band of interest, the corners of the CPW ground are truncated in a curved pattern. It is observed from the simulation results that the proposed UWB MM TA is resonating from 2.88 to 20 GHz, offering an impedance bandwidth of 17.12 GHz. In addition, acceptable radiation characteristics are observed in the proposed design, which makes it suitable for indoor wireless infrastructure.
D	**Journal Article(s)**
15.	2D-3D heterostructure of PtS2-x/Ga2O3 and their band alignment studies for high performance and broadband photodetector **G Bassi, D Kaur, R Dahiya, M Kumar** - Nanotechnology, 2024 **Abstract**: For deep ultraviolet (UV-C) photodetectors, Gallium oxide (Ga2O3) is a suitable candidate owing to its intrinsic ultra-wide band gap and high stability. However, its detection is limited within the UV-C region, which restricts it to cover a broad range, especially in visible and near-infrared (NIR) region. Therefore, constructing a heterostructure of Ga2O3 with an appropriate material having a narrow band gap is a worthwhile approach to compensate for it. In this category, PtS2 group-10 transitional metal dichalcogenide (TMDC) stands at the top owing to its narrow band gap (0.25-1.65 eV), high mobility, and stability for heterostructure synthesis. Moreover, heterostructure with Ga2O3 sensing in UV and PtS2 broad response in visible and IR range can broaden the spectrum from UV to NIR and to build broadband photodetector. In this work, we fabricated a 2D-3D PtS2-x/Ga2O3 heterostructure based broadband photodetector with detection from UV-C to NIR region. In addition, the PtS2-x/Ga2O3 device shows a high responsivity of 38.7 AW 1 and detectivity of 4.8×1013 Jones under 1100 nm light illumination at 5V bias. A fast response of 90 ms /86 ms illustrates the device's fast speed. An interface study between the PtS2-x and Ga2O3 was conducted using X-ray photoelectron spectroscopy and Ultraviolet photoelectron spectroscopy (UPS) which confirmed type-I band alignment. Finally, based on their band alignment study, a carrier transport mechanism was proposed at the interface. This work offers a new opportunity to fabricate large-area high-performance 2D-3D heterostructures based photodetectors for future optoelectronics devices.
16.	A mathematical framework for analysing particle flow in a network with multiple pools

	A Jain, AK Gupta - Royal Society Open Science, 2024 **Abstract**: In many real-world systems, the entry rate of particles into a lane is affected by the occupancy of nearby pools. For instance, in biological networks, the concentration of molecules on the side of a membrane affects the entry of particles through the membrane. To understand the behaviour of such networks, we develop a network model of ribosome flow models (RFMs) having multiple pools where each RFM captures the dynamics of particle flow in a lane and competes for the finite resources present at the nearby pool. We study a ribosome flow model network with two pools (RFMNTP) and show that the network always admits a steady state. We then analyse the behaviour of the RFMNTP with respect to modifying the transition rate through a theoretical framework. Simulations of the RFMNTP demonstrate a counterintuitive result. For example, increasing any of the transition rates in the presence of a slow site in an RFM can increase the output rate of some RFMs and decrease the output rate of the other RFMs simultaneously. This suggests that the role of local sharing of particles incorporated is non-trivial. Finally, we illustrate how these results can provide insights into studying a network with multiple pools.
17.	A multifaceted look at Garhwal Himalayan Glaciers: Quantifying area change, retreat, and mass balance, and its controlling parameters **S Guha, RK Tiwari,** G Zhang - Environment, Development and Sustainability, 2024 **Abstract:** Assessing glaciers' response to climate change is vital for water resource management. This study investigates changes in glacier areas, retreats and mass balance in the Garhwal Himalayan region. Initially, multitemporal Landsat imagery was used to delineate sample glacier boundaries for different study years manually. Subsequently, the Friedman test was employed to assess glacier area changes and retreats' temporal status across the Garhwal Himalayan region. The findings reveal a 1.12% deglaciation rate, consistent across observation periods. Mean area change for the first (2001-11), second (2011-16), and third epochs (2016-21) range from − 0.053 to -0.203, -0.084 to -0.309, and − 0.088 to -0.257%yr− 1, respectively. Glacier retreat also shows homogeneous length loss across all epochs, with mean scores ranging from 7.024 to 14.65, 7.87 to 17.03, and 8.956 to 14.98 myr− 1, respectively. Mass balance ranges from − 0.547 to -1.089 m.w.e.yr− 1 between 2000 and 2020, influenced by variations in mean slope and debris cover on individual glaciers. Debris cover and glacier slope are identified as key determinants, with debris cover exhibiting a positive coefficient and glacier slope demonstrating an inverse relationship with mass balance. Additionally, a 10% increase in debris cover corresponds to a 0.36 m.w.e.yr− 1 mass gain for a given slope, while a 10% increase in slope steepness results in a 0.86 m.w.e.yr− 1 mass loss for a given debris cover. The study highlights that glacier area doesn't affect the heterogeneous response. Instead, a strong correlation exists between glacier area and debris cover, with debris cover playing a key role in characterizing responses to changing climates. Thus, glacier area serves effectively as a proxy for debris cover extent.
18.	A universal-input on-board charger integrated power converter for switched reluctance motor drive based EV applicationsa **G Kumawat, V Shah, S Payami** - IEEE Transactions on Industry Applications, 2024 **Abstract:** In this article, the implementation of an integrated power converter (IPC) for a switched reluctance motor (SRM) drive is presented for electric vehicle (EV) applications. During driving mode, the proposed IPC is reconfigured as a modified asymmetric half-bridge (AHB) converter for SRM drive. During battery charging mode via a residential/public outlet, i.e., AC level-1 and AC level-2 charging, the proposed IPC is reutilized as an integrated on-board charger (OBC) by reconfiguring it into an interleaved buck cascaded buck-boost (IBuCBB) converter. The charging inductors for the IBuCBB configuration are realized via the phase windings of the SRM. Thus, the proposed IPC eliminates the requirement of an additional circuit for battery charging purposes. The integrated OBC facilitates battery charging over a universally

	available input voltage range, i.e., 85-265 Vrms (root mean square), with acceptable performance and efficiency. In addition, the proposed IPC configuration results in zero torque production instantaneously from the current within the phase windings during battery charging operation. Detailed theoretical analysis and experimental verification on a prototype 4-phase SRM are presented to evaluate the proposed IPC's driving and on-board battery charging features.
19.	Addition of magnetite nanoparticles and chitin biopolymer powders into the ambient sandy loam soil for the effective removal of Cr(VI): Batch adsorption and optimization study by response surface methodology **S Ganguly, S Ganguly** - Advanced Powder Technology, 2024 **Abstract:** This study features the development of a suitable composite for the effective removal of Cr(VI), a major carcinogenic heavy metal released from several anthropogenic sources. Firstly, the lithology of the study area was obtained from the Electrical Resistivity Tomography (ERT) survey and the ambient soil collected from the study was used as the major adsorbent. The composite was prepared by incorporating magnetite nanoparticles synthesized by the co–precipitation method and commercial chitin biopolymer powders into the ambient sandy loam soil. Several characterization studies were conducted to determine the surface morphology and the chemical composition of the adsorbents; the average particle diameter obtained for the composite and the magnetite nanoparticles was 32.78 μm and 28.50 nm, respectively. Next, the optimal adsorption efficiency of the composite was determined by the single–factor batch adsorption study. The effects of crucial parameters like dose, pH, contact time, and the initial concentration of Cr(VI) on the adsorption mechanism were investigated. The Box–Behnken Design (BBD) of the Response Surface Methodology (RSM) was further used to predict the interactions among the various parameters. The Analysis of Variance (ANOVA) was conducted to check the adequacy of the BBD model and a suitable 2nd – order quadratic equation was generated to calculate the expected adsorption efficiency. Among the adsorption isotherm models, the Langmuir adsorption model predicted the adsorption mechanism most accurately and the intraparticle diffusion model determined the rate–limiting steps of the adsorption mechanism effectively.
20.	Adipose tissue macrophage–derived microRNA-210-3p disrupts systemic insulin sensitivity by silencing GLUT4 in obesity **D Patra, P Ramprasad,** S Sharma… **D Pal** - Journal of Biological Chemistry, 2024 **Abstract:** Management of chronic obesity-associated metabolic disorders is a key challenge for biomedical researchers. During chronic obesity, visceral adipose tissue (VAT) undergoes substantial transformation characterized by a unique lipid-rich hypoxic AT microenvironment which plays a crucial role in VAT dysfunction, leading to insulin resistance (IR) and type 2 diabetes. Here, we demonstrate that obese AT microenvironment triggers the release of miR-210-3p microRNA-loaded extracellular vesicles from adipose tissue macrophages, which disseminate miR-210-3p to neighboring adipocytes, skeletal muscle cells, and hepatocytes through paracrine and endocrine actions, thereby influencing insulin sensitivity. Moreover, EVs collected from Dicer-silenced miR-210-3p–overexpressed bone marrow‐derived macrophages induce glucose intolerance and IR in lean mice. Mechanistically, miR-210-3p interacts with the 3′-UTR of GLUT4 mRNA and silences its expression, compromising cellular glucose uptake and insulin sensitivity. Therapeutic inhibition of miR-210-3p in VAT notably rescues high-fat diet–fed mice from obesity-induced systemic glucose intolerance. Thus, targeting adipose tissue macrophage–specific miR-210-3p during obesity could be a promising strategy for managing IR and type 2 diabetes.
21.	Aerodynamic performance and flow mechanism of 3D flapping wing using discrete vortex method **R Kumar, SS Padhee, D Samanta** - Journal of Fluids and Structures, 2024

	Abstract: In this work, we have performed numerical simulations of the flapping motion of a rectangular wing in a three-dimensional flow field using the discrete vortex method (DVM). The DVM method is computationally more convenient because it does not require the generation of a grid for the flow field at each time step as in other conventional simulation methods. In addition to the rigid wing case, the aerodynamic characteristics of a deformable wing are also investigated. The deformable wing is studied in various configurations, such as bending, twisting, and bending-twisting coupling (BTC), to provide a comprehensive analysis of its performance. In this study, we have introduced a novel aerodynamic technique in wing twisting. Unlike traditional wing rotation about a fixed root axis, our approach involves rotating the wing about a dynamically adjusted point located at the root of the leading edge. This novel approach was found to be effective in increase in the requisite aerodynamic force. The BTC wing represents reflects a sophisticated aerodynamic approach that optimally coordinates both twisting and bending deformations of the wing, resulting in a substantial improvement in its overall aerodynamic efficiency. The investigation of all four modes involves a detailed analysis of the flow mechanisms and vortex dynamics, which play a crucial role in influencing the aerodynamic forces, namely lift and thrust. The study aims to understand how these flow patterns change under different operating conditions and how these changes impact the generation of lift and thrust. The lift, thrust, and propulsive efficiency of all four modes are compared to provide a detailed understanding of their aerodynamic characteristics. The bent wing showed minimal improvements in lift and thrust compared to the rigid wing. In contrast, the twisted wing showed greater improvements in both lift and thrust. The BTC wing proves to be the most efficient method to improve aerodynamic performance during flapping. The parametric dependence of kinematic parameters such as asymmetric ratio (downstroke speed to upstroke speed), aspect ratio and reduced frequency on the aerodynamic performance was also investigated.
22.	Age-of-information based multi-UAV trajectories using deep reinforcement learning **A Kaur, SS Jha** - IETE Technical Review, 2024 **Abstract:** The use of unmanned aerial vehicles (UAVs) as a unified platform for sensing and communication is especially relevant in environments with inadequate infrastructure. In this paper, a multi-UAV system is constructed for dynamic data collection in a resource-constrained environment. The devised approach involves the implementation of an access platform referred to as the Access UAV (A_UAV). This A_UAV orchestrates the data collection process from Inspection-UAVs (I_UAVs), each equipped with a visual sensor, facilitating the relay of collected data to the cloud. Our approach jointly considers the trajectory scheduling of A_UAV and I_UAV to collect data from specific points in a decentralized manner. Specifically, a Deep Reinforcement Learning framework utilizing an actor-critic network is formulated for A_UAV, aiming to generate an equitable access schedule for I_UAVs. Moreover, trajectory scheduling of A_UAV ensures dynamic data collection while minimizing total system energy and the Age of Information (AoI) of data arriving from I_UAVs. The simulation results validate the performance of our proposed approach against several baselines under different parameter settings.
23.	‘All the same under the skin’: representations of class and gender in Michel Faber’s Under the Skin **M Jha, A Louis** - Journal of Gender Studies, 2024 **Abstract:** The essay, broadly conceived in two sections, examines the relationship between gender and class in Michel Faber’s novel Under the Skin. The first section utilizes Beverley Skeggs’ ethnography on working-class women in Britain to outline Isserley’s social positioning and how it is associated with negative value. We contend that Isserley’s appearance and employment reproduce the dominant and pathologizing cultural representations of working-class women. Further, the essay argues that Isserley disidentifies as a working-class woman through the discourse of improvement since the representations of her positioning constantly devalue her.

	In the second section, we shift our focus to the intersection of gender and class in the construction of masculine identity. We argue that the representation of men in the novel replicates that of working-class men in the British context. The essay draws on R.W. Connell's concept of marginalized masculinities to explore how the lives of men become inferior not just in terms of their bodies but also by failing to align with the hegemonic norms of manhood, such as staying employed, married, and being a provider for the family.
24.	An encyclopedic compendium on chemosensing supramolecular metal-organic gels **A Sharma**, N Kaur, **N Singh** - Chemistry: An Asian Journal, 2024 **Abstract:** Chemosensing, an interdisciplinary scientific domain, plays a pivotal role ranging from environmental monitoring to healthcare diagnostics and (inter)national security. Metal-organic gels (MOGs) are recognized for their stability, selectivity, and responsiveness, making them valuable for chemosensing applications. Researchers have explored the development of MOGs based on different metal ions and ligands, allowing for tailored properties and sensitivities, and have even demonstrated their applications as portable sensors such as paper-based test strips for practical use. Herein, several studies related to MOGs development and their applications in the chemosensing field via UV-visible or luminance along with electrochemical approach are presented. These papers explored MOGs as versatile materials with their use in sensing bio or environmental analytes. This review provides a foundational understanding of key concepts, methodologies, and recent advancements in this field, fostering the scientific community.
25.	An evaluation of the xenobotic cognitive project: Towards Stage 1 of xenobotic cognition **R Joy** - Endeavour, 2023 **Abstract**: Xenobot, the world's first biological robot, puts numerous philosophical riddles before us. One among them pertains to the cognitive status of these entities. Are these biological robots cognitive? To evaluate the cognitive status of xenobots and to resolve the puzzle of a single mind emerging from smaller sub-units, in this article, I juxtapose the cognitive capacities of xenobots with that of two other minimal models of cognition, i.e., basal cognition and nonliving active matter cognition. Further, the article underlines the essential cognitive capabilities that xenobots need to achieve to enter what I call stage 1 of xenobotic cognition. Stage 1 is characterized by numerous cognitive mechanisms, which are integral for the survival and cognition of basal organisms. Finally, I suggest that developing xenobots that can reach Stage 1 can help us achieve sophistication in the areas of evolution of the human mind, robotics, biology and medicine, and artificial intelligence (AI).
26.	Broken seniority symmetry in the semimagic proton mid-shell nucleus B Das, B Cederwall…**A Sharma**… - Physical Review Research, 2024 **Abstract:** Lifetime measurements of low-lying excited states in the semimagic (N=50) nucleus 95Rh have been performed by means of the fast-timing technique. The experiment was carried out using γ-ray detector arrays consisting of LaBr3(Ce) scintillators and germanium detectors integrated into the DESPEC experimental setup commissioned for the Facility for Antiproton and Ion Research (FAIR) Phase-0, Darmstadt, Germany. The excited states in 95Rh were populated primarily via the β decays of 95Pd nuclei, produced in the projectile fragmentation of a 850 MeV/nucleon 124Xe beam impinging on a 4g/cm29Be target. The deduced electromagnetic E2 transition strengths for the γ-ray cascade within the multiplet structure depopulating from the isomeric $I\pi$=21/2+ state are found to exhibit strong deviations from predictions of standard shell model calculations which feature approximately conserved seniority symmetry. In particular, the observation of a strongly suppressed E2 strength for the 13/2+→9/2+ ground state transition cannot be explained by calculations employing standard interactions. This remarkable result may require revision of the nucleon-nucleon interactions

	employed in state-of-the-art theoretical model calculations, and might also point to the need for including three-body forces in the Hamiltonian.
27.	Calix decorated ZnO nanohybrid material based smart portable electrochemical device for on-site analysis of diethylchlorophosphate R Kaur, G Bhardwaj, **G Singh**, N Kaur, **N Singh** - ACS Applied Nano Materials, 2024 **Abstract:** Chemical warfare agents (CWAs) pose a severe threat to both civilians and military personnel due to their extreme toxicity. The urgent necessity of creating a portable device for rapid on-site quantification of CWAs is evident. This article presents the design and synthesis of a specialized material, calix[4]pyrrole R2 modified zinc oxide nanohybrid material (R2-ZnO), and its utilization in crafting a smart portable electrochemical device (SPED). The detection capability of the R2-ZnO nanohybrid material was evaluated using various electrochemical techniques, specifically targeting the identification of CWAs' mimic compound, diethyl chlorophosphate (DCP). Upon interaction with the R2-ZnO nanohybrid material, DCP gets entrapped within the pyrrolic cavity of the R2-ZnO nanohybrid material and transforms into hydrolyzed, nontoxic compounds, resulting in a significant increase in current intensity. The interaction of DCP with the R2-ZnO nanohybrid material generates a quick response by enhancing the remarkable current density of the material. Surprisingly, when the R2-ZnO nanohybrid material was exposed to other organophosphates, there was no observable change in the current. Additionally, the developed SPED was tailored for the quantification of DCP, demonstrating fast response times within seconds of exposure. This pioneering research offers a promising pathway to develop a cost-effective, portable device for the rapid on-site quantification of hazardous CWAs.
28.	Can local heating and molecular crowders disintegrate amyloid aggregates? **N Kumar**, P Khatua, **SK Sinha** - Chemical Science, 2024 **Abstract**: The present study employs a blend of molecular dynamics simulations and a theoretical model to explore the potential disintegration mechanism of a matured Aβ octamer, aiming to offer a strategy to combat Alzheimer's disease. We investigate local heating and crowding effects on Aβ disintegration by selectively heating key Aβ segments and varying the concentration of sodium dodecyl sulphate (SDS), respectively. Despite initiation of disruption, Aβ aggregates resist complete disintegration during local heating due to rapid thermal energy distribution to the surrounding water. Conversely, although SDS molecules effectively inhibit Aβ aggregation at higher concentration through micelle formation, they fail to completely disintegrate the aggregate due to the exceedingly high energy barrier. To address the sampling challenge posed by the formidable energy barrier, we have performed well-tempered metadynamics simulations. Simulations reveal a multi-step disintegration mechanism for the Aβ octamer, suggesting a probable sequence: octamer → pentamer/hexamer ⇌ tetramer → monomer, with a rate-determining step constituting 45 kJ mol−1 barrier during the octamer to pentamer/hexamer transition. Additionally, we have proposed a novel two-state mean-field model based on Ising spins that offers an insight into the kinetics of the Aβ growth process and external perturbation effects on disintegration. Thus, the current simulation study, coupled with the newly introduced mean-field model, offers an insight into the detailed mechanisms underlying the Aβ aggregation process, guiding potential strategies for effective disintegration of Aβ aggregates.
29.	Cation-π-induced mixed-matrix nanocomposite for the detection and removal of Hg2+ and azinphos-methyl towards environment remediation† **K Kaur, G Singh,** N Kaur**, N Singh** - Environmental Science: Water Research & Technology, 2024 **Abstract:** The unregulated use of pesticides, which constitutes organophosphates, demands their

	continuous monitoring from a human health perspective. The development of efficient, reliable and affordable methods for the effective quantification, removal and detoxification of pesticides is indeed a significant challenge in the fields of agriculture, environmental science and public health. Herein, we designed a simple approach for the construction of a functionalised electrochemical material that includes the following steps: (i) the cation–π induced non-covalent functionalization of multiwalled carbon nanotubes (MWCNTs) with an organic cation IL, and (ii) the complexation of IL@MWCNTs with Hg2+ to accelerate electron transfer, apparently enhancing the response of Hg/IL@MWCNTs towards azinphos-methyl, as revealed by cyclic voltammetry. Hg/IL@MWCNTs/GCE exhibits electrocatalytic behaviour towards azinphos-methyl (AZM) with a low detection limit of 1.10 μM and a wide linear range (0.20–180 μM). The degradation of the AZM pesticide was supported by 31P NMR titration and mass spectrometry, which confirmed the conversion of AZM into its non-toxic products. Taking into account the aforementioned findings, the functionalised IL@MWCNT composite was fabricated into an ultrathin polyamide layer on a PES support membrane via interfacial polymerisation for practical application. The developed nanocomposite membrane removes the Hg2+ metal ion and azinphos-methyl pesticide from contaminated water with a removal efficiency of 95% and 90%, respectively. 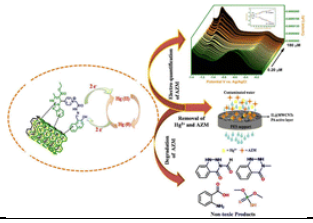
30.	Copper-catalyzed chemoselective o-arylation of oxindoles: access to cyclic aryl carboxyimidates PR Singh, M Lamba, **A Goswami** - The Journal of Organic Chemistry, 2024 **Abstract:** We have developed a highly efficient base- and additive-free chemoselective CuO-catalyzed strategy for the O-arylation of 2-oxindoles to synthesize 2-phenoxy-3H-indole and 2-phenoxy-1H-indole derivatives in the presence of diaryl iodonium salts. This method offers a variety of O-arylated oxindoles in good to excellent yields under relatively milder reaction conditions. Furthermore, this methodology was extended for the O-arylation of 2-pyridinone and isoindoline-1-one derivatives as well. 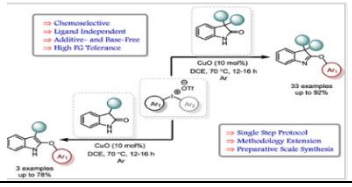
31.	Covalent organic framework bifunctional catalyst for glucose oxidation reaction coupled nitrate to ammonia electrolysis **A Chaturvedi**… **S Kaur, TC Nagaiah**… - ACS Energy Letters, 2024 **Abstract:** Ammonia is a crucial feedstock for the chemical industry, a carbon-free energy source, and a safe source for hydrogen storage. The electrochemical nitrate reduction reaction (NO3RR) is one promising strategy for greener ammonia synthesis due to high water solubility and low N═O bond dissociation energy of NO3–. More importantly, polluted water is a source of NO3–. Herein, we rationally designed a bifunctional covalent organic framework catalyst (Ru-Tta-Dfp) having a triazine- and pyridine-rich backbone with inherent Ru-nanocluster sites to control both NO3– and H+ diffusion and interactions to achieve selective conversion of NO3– to ammonia monitored by operando Raman spectroscopy (93.93% faradaic efficiency and yield rate of 1.16 mg h–1cm–2 at −0.4 V vs RHE). Moreover, we have developed a strategy for the first time to couple the anodic glucose oxidation reaction (GOR) to facilitate the cathodic NO3RR with reduced energy consumption and to achieve value-added products at both electrodes. Notably,

	NO3RR-GOR full cell studies generate a ~2.5 times higher NH3 yield rate than that of NO3RR-OER.
32.	Cover feature: Ni nanoparticles supported montmorillonite clay for selective catalytic transfer hydrodeoxygenation of vanillin into 2-methoxy-4-methylphenol (ChemCatChem 9/2024) **A Kumar**, R Bal, **R Srivastava** - ChemCatChem, 2024 **Abstract**: The Cover Feature illustrates the conversion of lignocellulosic biomass-derived, lignin bio-oil compound, Vanillin (VAN), to 2-methoxy-4-methylphenol (MMP), a promising candidate for future biofuel applications for its use in fragrances and intermediate in pharmaceutical synthesis, via transfer hydrodeoxygenation. In their Research Article, R. Srivastava et al. reveal Ni nanoparticle (NP)-loaded montmorillonite (MMT) clay catalysts in catalytic transfer hydrodeoxygenation of lignin bio-oil compounds with isopropanol as a hydrogen source under mild conditions. Ni(10%)/MMT yields MMP with high conversions and selectivity, showcasing impressive recyclability, stability, and efficacy. Optimal Ni NPs and MMT acidity balance influences catalysis. The Ni(10%)/MMT catalyst outperforms reported Ni NP-based catalysts in VAN conversion and MMP selectivity, offering a greener approach to chemical production and advancing eco-friendly catalytic technologies.
33.	Cyano disubstituted tetrabenzoindeno[2,1-a]fluorene: open-shell or closed-shell? **PK Sharma**, P Jana, S Bandyopadhyay, **S Das** - Chemical Communications, 2024 **Abstract**: Organic diradicaloids have lately emerged as potential spintronic materials. We report the unprecedented synthesis of a near-IR absorbing indeno[2,1-a]fluorene derivative that displays remarkably low LUMO (−4.15 eV) and a small HOMO–LUMO gap (0.85 eV). NMR/EPR studies indicated its open-shell diradical property, which was supported by DFT calculations while suggesting a 30% diradical character and a small singlet (S)–triplet (T) gap (−2.52 kcal mol−1). A large bond length alternation of the as-indacene core for its single-crystals indicated a quinoidal contribution with greater antiaromaticity, which is in line with the small diradical character despite showing a small S–T gap. 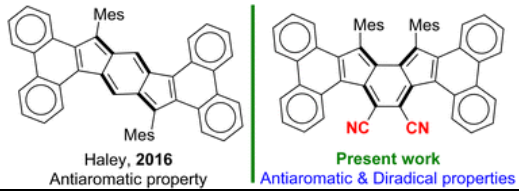
34.	Deep learning approach for gait detection for precise stimulation of FES to correct foot drop **B Basumatary, RS Halder, C Singhal, AN Mallick…AK Sahani** - IETE Technical Review, 2024 **Abstract:** Automatic detection of foot lift is one of the most important events of Functional Electrical Stimulation (FES). The FES system is used for the correction of Foot Drop (FD). FD is a condition where a person is unable to lift their foot from the ground due to complications that may arise after a stroke or spinal cord injury. It is crucial to accurately detect the patient's foot lift event when correcting FD through FES as the pulse should only be applied when the person lifts their foot. The FES system applies the electrical pulse based on the input of the foot-lift detection sensor. A conventional FES system employs a sensor that is affixed on the heel to detect the lifting of the foot, but the connecting cables make the patient uncomfortable. To address this problem, IMU (Inertial Measurement Unit)-based sensors have been used, but they have some disadvantages, such as false triggering, low accuracy, and calibration. In this paper, we have presented an algorithm for detecting foot-lift events with high accuracy using a single IMU sensor through the application of deep learning techniques. We have recorded data from 10 healthy people and 10 foot drop patients. We have implemented Artificial Neural Network

	(ANN), K-Nearest Neighbour (KNN), and Convolutional Neural Network (CNN) models on these data and compared the results of these three models. The proposed algorithm aims to improve the precision of stimulation in the FES system.
35.	Design of 2D half-metallic CoAl2S4 with robust ferromagnetism and high Curie temperature H Lahraichi , M Kibbou…**R Ahuja**… - Journal of Magnetism and Magnetic Materials, 2024 **Abstract:** Two-dimensional 2D ferromagnetic materials featuring intrinsic half-metallicity (HM) and high critical temperature Tc emerge as promising candidates for innovative low-dimensional spintronic devices. In this study, we employ first-principles calculations to predict a novel 2D half-metallic ferromagnet CoAl2S4 monolayer, a member of the layered $AB2X4$ family. The material's energetic, mechanical, and dynamical stability is affirmed through analyses of its cohesive energy, elastic constants, and phonon spectrum, respectively. The ferromagnetic behavior observed in CoAl2S4 can be explained by the superexchange interaction of Co-S-Co bonds, consistent with the Goodenough–Kanamori rules. Notably, CoAl2S4 displays robust ferromagnetism with a Curie temperature reaching up to 435 K. The band structures show a large half-metal gap (2.83 eV), ensuring the stability of the half-metallic state. Additionally, the CoAl2S4 monolayer demonstrates a preferential easy magnetization along the out-of-plane direction. Consequently, the rich CoAl2S4 monolayer is expected to boost advancements in spintronics, magnetostrictive materials, and magnetic memory devices.
36.	Design of porphyrin-based frameworks for artificial photosynthesis and environmental remediation: Recent progress and future prospects **R Das,** PK Verma, **CM Nagaraja** - Coordination Chemistry Reviews, 2024 **Abstract:** Porphyrins constitute the central part of various catalytic processes in natural systems, and mimicking these processes using synthetic porphyrins and metalloporphyrins is a fascinating area of biomimetic catalysis. Consequently, porphyrins are widely studied tetrapyrrolic frameworks encompassing interesting photochemical, photophysical, and photoredox properties. Hence, porphyrins are utilized as promising catalysts for diverse catalytic transformations, including water splitting, CO2 reduction, and environmental remediation applications. However, applying porphyrin molecules as catalysts restricts their catalytic efficiency due to self-aggregation and poor structural rigidity. Transforming the monomeric units into extended (2D/3D) networks trounces their aggregation-related limitations, makes them highly efficient catalytic materials, and diversifies their catalytic applicability. Besides, porphyrin-based frameworks serve as excellent light-harvesting or resonance energy transfer functional struts and facilitate efficient photocatalytic transformations. Herein, the research progress in developing porphyrin-based frameworks assembled from various porphyrin building blocks for artificial photosynthesis, viz water splitting to H2 generation, photoreduction of CO2, and environmental remediation, is presented comprehensively. Notably, the mechanistic aspects of the photocatalytic processes catalyzed by porphyrin-based frameworks are discussed. Finally, the current challenges and perspectives are highlighted, providing ideas for designing highly efficient porphyrin frameworks for energy and environmental applications. 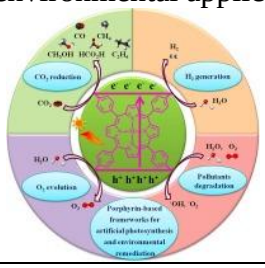
37.	Diradical polar reactivity induced by electricity-mediated ground state triplet nitrenium species **N Banerjee, A Kushwaha, S Dutt, D Saha, TJD Kumar, P Banerjee** - Advanced Synthesis & Catalysis, 2024

	Abstract: It is extremely rare for reactive intermediates to possess a ground state triplet character. Excited state triplet intermediates are generally accessed by means of photon transfer from a tunable light source or by using any triplet sensitizers. N-acyl N-alkoxy nitreniums are an important class of reactive intermediates in the synthetic organic community due to their prolonged lifetime and ground-state singlet character. Herein, we report an external oxidant and toxic catalyst-free mild electrochemical protocol to access nitrenium reactive intermediate. Experimental findings of the mechanistic pathway suggested a theoretically predicted triplet reactive intermediate that is energetically favorable to the singlet pathway.
38.	Dynamic hierarchical intrusion detection task offloading in IoT edge networks **M Sahi, N Auluck,** A Azim, MA Maruf - Software - Practice and Experience, 2024 **Abstract:** The Internet of Things (IoT) has gained widespread importance in recent time. However, the related issues of security and privacy persist in such IoT networks. Owing to device limitations in terms of computational power and storage, standard protection approaches cannot be deployed. In this article, we propose a lightweight distributed intrusion detection system (IDS) framework, called FCAFE-BNET (Fog based Context Aware Feature Extraction using BranchyNET). The proposed FCAFE-BNET approach considers versatile network conditions, such as varying bandwidths and data loads, while allocating inference tasks to cloud/edge resources. FCAFE-BNET is able to adjust to dynamic network conditions. This can be advantageous for applications with particular quality of service requirements, such as video streaming or real-time communication, ensuring a steady and reliable performance. Early exit deep neural networks (DNNs) have been employed for faster inference generation at the edge. Often, the weights that the model learns in the initial layer may be sufficiently qualified to perform the required classification tasks. Instead of using subsequent layers of DNNs for generating the inference, we have employed the early-exit mechanism in the DNNs. Such DNNs help to predict a wide range of testing samples through these early-exit branches, upon crossing a threshold. This method maintains the confidence values corresponding to the inference. Employing this approach, we achieved a faster inference, with significantly high accuracy. Comparative studies exploit manual feature extraction techniques, that can potentially overlook certain valuable patterns, thus degrading classification performance. The proposed framework converts textual/tabular data into 2-D images, allowing the DNN model to autonomously learns its own features. This conversion scheme facilitated the identification of various intrusion types, ranging from 5 to 14 different categories. FCAFE-BNET works for both network-based and host-based IDS: NIDS and HIDS. Our experiments demonstrate that, in comparison with recent approaches, FCAFE-BNET achieves a 39.12%–50.23% reduction in the total inference time on benchmark real-world datasets, such as: NSL-KDD, UNSW-NB 15, ToN_IoT, and ADFA_LD.
39.	ECMAC: Edge-assisted cluster-based MAC protocol in software-defined vehicular NetworksECMAC: Edge-assisted cluster-based MAC protocol in software-defined vehicular networks Y Shen, J Jeong**, J Jun**, T Oh, Y Baek - IEEE Transactions on Vehicular Technology, 2024 **Abstract:** Vehicular networks have emerged as a promising means to mitigate safety hazards in modern transportation systems. On highways, emergency situations associated with vehicles necessitate a reliable media access control (MAC) protocol that can provide timely warnings of possible vehicle collisions. In this paper, we present an edge-assisted cluster-based MAC protocol (ECMAC) for packet dissemination in software-defined vehicular networks. To reduce the control messaging overhead for clustering, ECMAC separates the cluster control plane (i.e., managing cluster formation) from the data plane (i.e., actual data transmission and forwarding) by using a software-defined network controller in a cellular network edge server. For transmitting packets, we design a time-division multiple access (TDMA) schedule algorithm to guarantee a high reliability and a low latency. The TDMA schedule in ECMAC is determined by a joint optimization process in the cellular edge, which is formulated as a binary integer linear

	programming problem and solved by a heuristic approach based on the divide-and-conquer paradigm. This joint optimization process minimizes the signal interference by jointly considering channel assignment and time slot allocation, thereby ensuring reliable communication. Through extensive simulations, our performance results show that ECMAC improves the successful delivery ratio of emergency packets by at least 25 %, compared with state-of-the-art approaches.
40.	Effect of laser remelting on the microstructural and mechanical properties of high-velocity oxy-fuel (HVOF)-sprayed WC-NiCr coating NK Singh, **G Vinay, H Singh**, PP Bandyopadhyay - Journal of Thermal Spray Technology, 2024 **Abstract:** WC-based coatings are found efficient in providing excellent tribological properties to the structures and components subjected to harsh wear and erosion environments. High-velocity oxy-fuel (HVOF) spraying is known as one of the best techniques to deposit such coatings. However, there still exists scope for further microstructural refinement and improvement in the mechanical properties of the as-sprayed HVOF coatings. Laser remelting has proven to be an appropriate process to achieve such improvement in as-sprayed WC-based coatings. In the current investigation, laser remelting at two different power levels was done on the HVOF-sprayed WC-NiCr coating on stainless steel specimens. The post-processed coatings were analyzed using a scanning electron microscope, x-ray diffraction, x-ray photoelectron spectroscopy, and ImageJ software to study the microstructural changes. Microhardness and surface roughness measurements were also performed to study the mechanical changes. The laser remelting resulted in a smoother coating surface, having lower porosity, lower surface roughness, and higher microhardness as compared to the as-sprayed HVOF coatings. The highest reduction in the porosity was found to be around 72%, whereas, an increment of around 21% in the microhardness was witnessed. These two parameters are crucial for the tribological performance of the coatings. The current study also gives direction to further study these remelted coatings in tribological conditions.
41.	Energy efficient heuristics to schedule task graphs on heterogeneous voltage-frequency islands Sanchit, A Jain, **J Singh**, N Singh - IETE Journal of Research, 2024 **Abstract:** For energy and cost-efficient computing, many desktops and embedded computing devices these days use voltage frequency islands (VFIs) based processors. An island in VFIs consists of multiple homogeneous cores; however, multiple islands are generally heterogeneous in nature. In contrary to architectures (non-VFI) with per-core dynamic voltage frequency scaling (DVFS), in VFI, all the cores in an island run on the same voltage/frequency at the same time. The energy-aware scheduling of task graphs on VFI architectures is challenging and different from non-VFI architectures in which task-based DVFS is possible. However, in VFI scheduling, the time slot for which an island runs on a particular voltage will be decided. In this paper, we analyse 20 different scheduling heuristics for VFI architectures by varying the size of this time slot based on the workload properties and also by varying the voltage/frequency of the time slots. We also propose a heuristic OptSlotVFI to utilize all the slots optimally. The results show that the VFI scheduling heuristics are able to generate schedules which improve energy consumption up to 25% with an equivalent or shorter schedule length than the state-of-the-art approaches.
42.	Enhancing formability in micro-incremental sheet forming by a novel stacking method of ultra-thin sheets **M Pal, A Agrawal, CK Nirala** - Manufacturing Letters, 2024 **Abstract**: Metallic foils are used extensively in the microelectronics and avionics industries. However, forming these foils into complex shapes is challenging, due to size-effect. The foils are susceptible to bending and distortion under self-weight as they lack stiffness and fail early during forming. Processes, like drawing, stamping, etc. have been explored at the micro-scale, but they

	are suitable for simpler geometry and low aspect ratio parts. Micro-incremental sheet forming (μISF) is a new flexible forming process that can be used for micro-scale deformation of foils into complex geometries with higher formability. This work attempts to improve the stiffness and formability of 100 μm thick CP-Ti Gr2 foils by proposing a unique 'stacking of foils' (SOF) approach in μISF. In SOF, multiple foils are stacked together which increases their stiffness and plastic deformation. Experimental results demonstrate that formability is considerably improved by about 21–27 %, with better geometrical accuracy of the micro-parts.
43.	Enhancing nitroaromatics reduction through synergistic participation of Ni NPs and nickel ferrite/C nanocomposite: A path towards greener industrial viability **GS More, S Kharb, P Gill, R Srivastav** - Applied Catalysis A: General, 2024 **Abstract:** Ni/Fe-citrate gel was reduced in an H2/Ar, forming Ni NPs decorated NiFe2O4-C for eco-friendly nitroaromatics reduction. In-depth characterization of the catalyst highlighted the synergistic interaction between Ni NPs and NiFe2O4 (Ni/NiFe2O4-C), achieving ~ 99 % conversion of nitroaromatics into amines at 70 °C and 0.5 MPa H2 in water. The cooperative effects of Ni NPs, NiFe2O4, and carbon were instrumental in enhancing the adsorption of hydrogen and nitroaromatics, and the kinetic study showed effectively reducing the activation barrier for the reduction. The HR-TEM, XPS, and H2-TPR provided valuable insights into the formation of Ni NPs and the NiFe2O4 framework, emphasizing their synergistic relationship. Raman spectroscopy and TGA analysis confirmed the formation of carbon. Remarkably, the highly active Ni/NiFe2O4-C catalyst recycled for five cycles without losing activity. *p*-Aminophenol on 7 g will receive significant attention, emphasizing the substantial promise of this sustainable transition metal-based catalyst for the eco-friendly hydrogenation of nitroaromatics. 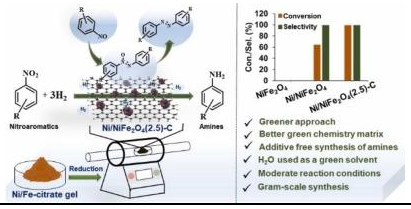
44.	Evaluation of the energy absorbing capacity of the two combinations of TPMS structure subjected to different compressive strain rates Technical Paper Published: 05 May 2024 AI Ansari, NA Sheikh, **N Kumar** - Journal of the Brazilian Society of Mechanical Sciences and Engineering, 2024 **Abstract:** This study provides an overview of the most recent advancements in the production of two triple periodic minimal (TPMS) structure combinations using acrylonitrile butadiene styrene (ABS-M30i) material, their structural mechanics, and energy absorption properties. The geometrical parameters of the three designs of TPMS foam structures with various densities were studied in accordance with the Gibson Ashby criteria, and the behavior of the structures in terms of energy absorption at strain rates of 1 s−1, 10 s−1, and 100 s−1 was performed. Mechanical assessment results for the three design structures were consistent with the Gibson–Ashby model assumptions, and Gibson–Ashby equations were developed to predict the mechanical performance of three different types of lattice structures generated by FDM. This study provides techniques for predicting the mechanical properties of two combination of TPMS structure such as (i) PrimaryIwp Schwarz Primitive (PSP), (ii) Neovius-SchwarzD (NS), and (iii) Gyroid-Fischerkoch structures made by FDM, as well as a better understanding of the possibilities and limitations of these structures. At three different strain rates, each of the three TPMS design structural crashworthiness features was successfully recognized, analyzed, and documented.
45.	Experimental investigations of heat transfer in simultaneously developing transitional regime of mixed convection flows in a vertical tube **S Gorai, D Samanta**, SK Das - ASME Journal of Heat and Mass Transfer, 2024

	Abstract: The study of flow behaviour in the simultaneously developing transitional regime of mixed convection flows is rare. It has been believed that the transitional regime will give a good compromise between pressure drop and heat transfer compared to laminar and turbulent flow regime. In this experimental study, the friction factor (f) and Nusselt number (Nu) characteristics for buoyancy-assisted and opposed flows of water in concurrently developing transitional regime of mixed convection through a vertical tube are studied. Experiments were done for Reynolds numbers (Re) varying from 500 to 15000, Grashof numbers (Gr) from 1.25×104 to 5×106, Prandtl numbers (Pr) from 3 to 7, and Richardson numbers (Ri) from 0 to 0.1 subjected to uniform heat flux boundary conditions. A flow visualization provision after the test section which confirms an early transition in buoyancy-opposing flow (Rec = 2264) compared to buoyancy-aiding flow (Rec = 2468) at a fixed Ri of 0.1. Further, with the increase in Ri from 0 to 0.1, the average f decreases, and the average Nu increases in both aiding and opposing flows. It confirms that, the onset of transition gets delayed with the increase of heat flux supplied in both the flows. Based on the present outcomes, an efficient heat exchanging device can be operated either to delay or advance the transition in a vertical pipe flow for optimum heat transfer.
46.	Fabrication of 208Pb and 193Ir targets on Al-backing using high/ultra-high vacuum deposition technique for low-energy nuclear reaction experiments **Amanjot, R Kaur, S Kumar, PP Singh** - Vacuum, 2024 **Abstract:** Aiming to study the interplay of different nuclear reactions at low incident energies, thin targets of enriched stable isotopes, 208Pb and 193Ir, have been fabricated at the target development laboratory of the Inter-University Accelerator Centre (IUAC), New Delhi. As a means of preparing a large number of thin isotopically pure targets, physical vapour deposition techniques, (a) resistive heating, for fabrication of 208Pb targets of mass thickness 160- /cm2, and (b) electron-gun evaporation technique, for fabrication of 193Ir targets of mass thickness 17- /cm2, have been employed. The fabricated targets were characterized using Rutherford Backscattering Spectrometry (RBS) and Field Emission Scanning Electron Microscopy (FE–SEM). The thickness of targets was estimated based on the evaporation rate and measured by RBS. The RBS was employed to analyse the samples for trace- and heavy impurities, provided the measurements and analysis suggest that the targets prepared in the present work do not contain any impurities. FE-SEM was employed to examine the surface morphology and microstructure in high resolution. This technique enables the detection of any morphological changes induced by the irradiation process, offering insights into the effects of irradiation on the target films. The targets have been successfully deployed to measure complete and incomplete fusion excitation functions, mass distribution of fission fragments, and forward ranges of target-like recoils in 12C + 208Pb, 193Ir reactions from sub- to above barrier energies. Preliminary data analysis suggests the achievement of high-quality 208Pb and 193Ir target foils.
47.	Forecasting stock indices: Stochastic and artificial neural network models **NK Pande, A Kumar, AK Gupta** - Computational Economics, 2024 **Abstract:** In recent years, there has been a bloom in the stock investors due to availability of various platforms that have provided an opportunity even for small scale investors to earn profits from the market. However, due to very high uncertainty, bad investments can lead to large financial losses and hence need for tools that can predict stock behaviour, arises. The main objective of this article is to provide a comparative empirical analysis of stochastic models with artificial neural networks in the prediction of stock indices across different markets. We consider three types of models, namely the time series models: autoregressive integrated moving average and autoregressive fractionally integrated moving average; jump diffusion models: Merton jump diffusion and Kou jump diffusion; the artificial neural network models: feed-forward network and the long short term memory. These models are used to forecast 10, 20 and 30 days ahead prices of major stock indices across different markets which include both developed and

	emerging economies. It is shown that the long short-term memory performs better than other considered models on most of the considered indices over all the time horizons. The results also indicate the forecasts provided by the LSTM model are significant from both statistical point of view and can possibly be used for profitable investments.
48.	Generalized fractional derivatives generated by Dickman subordinator and related stochastic processes N Gupta, **A Kumar**, N Leonenko, J Vaz - Fractional Calculus and Applied Analysis, 2024 **Abstract:** In this article, convolution-type fractional derivatives generated by Dickman subordinator and inverse Dickman subordinator are discussed. The Dickman subordinator and its inverse are generalizations of stable and inverse stable subordinators, respectively. The series representations of densities of the Dickman subordinator and inverse Dickman subordinator are also obtained, which could be helpful for computational purposes. Moreover, the space and time-fractional Poisson-Dickman processes, space-fractional Skellam Dickman process and non-homogenous Poisson-Dickman process are introduced and their main properties are studied.
49.	Geometric infinitely divisible autoregressive models **MS Dhull, A Kumar** - Statistical Papers, 2024 **Abstract:** In this article, we discuss some geometric infinitely divisible (gid) random variables using the Laplace exponents which are Bernstein functions and study their properties. The distributional properties and limiting behavior of the probability densities of these gid random variables at are studied. The autoregressive (AR) models with gid marginals are introduced. Further, the first order AR process is generalized to kth order AR process. We also provide the parameter estimation method based on conditional least square and method of moments for the introduced AR(1) process. We also apply the introduced AR(1) model with geometric inverse Gaussian marginals on the household energy usage data which provide a good fit as compared to normal AR(1) data.
50.	Geometric transformation of modified multiwalled carbon nanotubes-based heterometallic nanostructured material: a model for the electrochemical discrimination of insecticides R Kaur, G Bhardwaj, **N Singh,** N Kaur - Langmuir, 2024 **Abstract:** Multifunctional carbon-based materials exhibit a large number of unprecedented active sites via an electron transfer process and act as a desired platform for exploring high-performance electroactive material. Herein, we exemplify the holistic design of a heterometallic nanostructured material (MWCNTs@KR-6/Mn/Sn/Pb) formed by the integration of metals (Mn2+, Sn2+, and Pb2+) and a dipodal ligand (KR-6) at the surface of multiwalled carbon nanotubes (MWCNTs). First, MWCNTs@KR-6 was readily synthesized via a noncovalent approach, which was further sequentially doped by Mn2+, Sn2+, and Pb2+ to give MWCNTs@KR-6/Mn/Sn/Pb. The designed material showed excellent electrochemical activity for the discrimination of insecticides belonging to structurally different classes. In contrast to that of the individual building components, both the stability and electrochemical activity of heterometallic nanostructured material were remarkably enhanced, resulting in a magnificent electrochemical performance of the developed material. Hence, the current work reports a comprehensive synthetic approach for MWCNTs@KR-6/Mn/Sn/Pb synthesis by synergizing unique properties of the heterometallic complex with MWCNTs. This work also offers a new insight into the design of multifunctional carbon-based materials for discrimination of different analytes on the basis of their redox potential.

	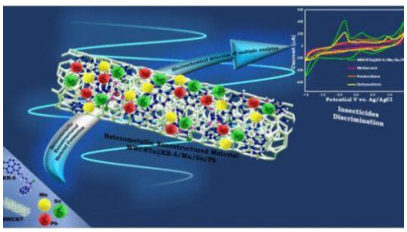
51.	Headroom-based frequency and DC voltage control for large disturbances in multi-terminal HVDC (MTDC) grids AS Kumar, **BP Padhy** - IEEE Transactions on Industry Applications, 2024 **Abstract:** In the AC-integrated MTDC (AC-MTDC) grids, regulating the DC voltage and frequency became indispensable for reliable and stable operation. For effective DC voltage and frequency regulation, Headroom-based Adaptive Droop Control (HR-ADC) has been proposed in this paper. The HR-ADC changes droop value adaptively based on the available headroom at Grid Side Voltage Source Converters (GSCs), Wind and solar form connected Voltage Source Converter stations, say Renewable Energy Side Voltage Source Converters (RECs). In the case of RECs, available power at the Wind or Solar Farms is also considered while operating in the proposed HR-ADC. This approach is autonomous and robust, ensuring the system operates stably and reliably even during significant disturbances in the AC-MTDC grids. A lower-order dynamic model-based eigenvalue and post-contingencies analysis of the AC-MTDC grid has been carried out to show the virtue of the proposed HR-ADC methodology. Further, to show the significance of the proposed method, it is compared with a conventional Fixed Droop Control (FDC) by considering the five terminal CIGRE Bi-polar DC grid benchmark model integrated into two area power systems. A PSCAD/EMTDC software is used to simulate this test system.
52.	High-resolution heteronuclear correlations between spin-1/2 and half-integer quadrupolar nuclei under fast MAS solid-state NMR **MK Pandey**, Y Nishiyama - Biophysical Chemistry, 2024 **Abstract:** High isotropic resolution is essential for the structural elucidation of samples with multiple sites. In this study, utilizing the benefits of TRAPDOR-based heteronuclear multiple quantum coherence (T-HMQC) and a pair of one rotor period long cosine amplitude modulated low-power (cos-lp) pulse-based symmetric-split-t1 multiple-quantum magic angle spinning (MQMAS) methods, we have developed a proton-detected 2D 35Cl/1H T-HMQC-MQMAS pulse sequence under fast MAS (70 kHz) to achieve high-resolution in the indirect dimension of the spin-3/2 (35Cl) nuclei connected via protons. As T-HMQC polarizes not only single-quantum central transition (SQCT) but also triple-quantum (TQ) coherences, the proposed 2D pulse sequence is implemented via selection of two coherence pathways (SQCT TQ SQCT and TQ SQCT TQ) resulting in the 35Cl isotropic dimension and is superior to the existing double-quantum satellite-transition (DQST) T-HMQC in terms of resolution.
53.	Immunosuppressive effects of morphine on macrophage polarization and function **JA Malik, MA Khan, T Lamba, MA Zafar, S Nanda…JN Agrewala** - European Journal of Pharmacology, 2024 **Abstract**: Macrophages play a pivotal role in safeguarding against a broad spectrum of infections, from viral, bacterial, fungal to parasitic threats and contributing to the immune defense against cancer. While morphine's immunosuppressive effects on immune cells are extensively documented, a significant knowledge gap exists regarding its influence on macrophage polarization and differentiation. Hence, we conducted a study that unveils that prior exposure to morphine significantly impedes the differentiation of bone marrow cells into macrophages. Furthermore, the polarization of macrophages toward the M1 phenotype under

	M1-inducing conditions experiences substantial impairment, as evidenced by the diminished expression of CD80, CD86, CD40, iNOS, and MHCII. This correlates with reduced expression of M1 phenotypical markers such as iNOS, IL-1β, and IL-6, accompanied by noticeable morphological, size, and phagocytic alterations. Further, we also observed that morphine affected M2 macrophages. These findings emphasize the necessity for a more comprehensive understanding of the impact of morphine on compromising macrophage function and its potential ramifications for therapeutic approaches.
54.	In-plan distribution of peak floor acceleration demands in torsionally irregular buildings **A Jain, M Surana** - Journal of Building Engineering, 2024 **Abstract:** The precise estimation of peak floor acceleration demands is essential to ensure the seismic safety of building contents and attachments. The present study aims to investigate the distribution of the peak floor acceleration demands across the floor plan in torsionally irregular buildings. To achieve this objective, 28 mid-rise reinforced concrete buildings with torsional irregularities are analyzed under 5600 bidirectional earthquake excitations, considering various strength ratios in buildings. A total of 2,59,200 in-structure amplification factors are estimated at multiple locations within the building plan and also at different floors. It is observed that current seismic design codes tend to underestimate the in-structure amplification factor for torsionally irregular buildings, particularly at locations distant from the center of rigidity (towards flexible frames), by up to 137 % for elastic buildings, and up to 54 % for moderately inelastic buildings. Even in the case of frames closer to the stiff frames, the seismic design codes underestimated the in-structure amplification factor by up to 68 % for elastic buildings. It is observed that a strong relationship exists between the torsional amplification of the peak floor acceleration and displacement amplification due to building torsion at the floor of interest. The torsional amplification of peak floor acceleration is found to be approximately equal to torsional displacement amplification for the flexible frames at the floor of interest. Simplified equations are developed for their integration with existing building codes to precisely estimate the in-plan distribution of peak floor acceleration demands in torsionally irregular buildings.
55.	Inverse problem assisted multivariate geostatistical model for identification of transmissivity fields **A Kapoor, D Kashyap** - Frontlers in water, 2024 **Abstract:** Groundwater models often require transmissivity (T) fields as an input. These T fields are commonly generated by performing univariate interpolation of the T data. This T data is derived from pumping tests and is generally limited due to the large costs and logistical requirements. Hence T fields generated using this limited data may not be representative for a whole study region. Groundwater models often require transmissivity (T) fields as an input. These T fields are commonly generated by performing univariate interpolation (using kriging, IDW etc.) of the T data. This T data is derived from pumping tests and is generally limited due to the large costs and logistical requirements. Hence, the T fields generated using this limited data may not be representative for the whole study region. This study presents a novel cokriging based methodology to generate credible T fields. Cokriging - a multivariate geostatistical interpolation method permits incorporation of additional correlated auxiliary variables for the generation of enhanced fields. Here abundantly available litholog derived saturated thickness data has been used as secondary (auxiliary) data given its correlation with the primary T data. Additionally, the proposed methodology addresses two operational problems of traditional cokriging procedure. The first operational problem is the poor estimation of variogram and cross-variogram parameters due to sparse T data. The second problem is the determination of relative contributions of primary and secondary variable in the estimation process. These two problems have been resolved by proposing a set of novel non-bias conditions, and linking the interpolator with a head based inverse problem solution for credible estimation of these parameters. The proposed methodology has been applied to Bist doab region in Punjab (India). Additionally, base

	line studies have been performed to elucidate the superiority of the proposed cokriging based methodology over kriging in terms of head reproducibility. Copyright © 2024 Kapoor and Kashyap.
56.	It takes two to negotiate: Modeling social exchange in online multiplayer games K Jaidka, **H Ahuja**, LHX Ng - Proceedings of the ACM on Human-Computer Interaction, 2024 **Abstract:** Online games are dynamic environments where players interact with each other, which offers a rich setting for understanding how players negotiate their way through the game to an ultimate victory. This work studies online player interactions during the turn-based strategy game, Diplomacy. We annotated a dataset of over 10,000 chat messages for different negotiation strategies and empirically examined their importance in predicting long- and short-term game outcomes. Although negotiation strategies can be predicted reasonably accurately through the linguistic modeling of the chat messages, more is needed for predicting short-term outcomes such as trustworthiness. On the other hand, they are essential in graph-aware reinforcement learning approaches to predict long-term outcomes, such as a player's success, based on their prior negotiation history. We close with a discussion of the implications and impact of our work.
57.	Mechanism of DSA effect correlating to the macroscopic PLC banding in high-Mn austenitic steel S Hwang, MH Park, Y Bai, **A Lavakumar**…- Scripta Materialia, 2024 **Abstract:** Mechanism of dynamic strain aging (DSA) effect in high-Mn austenitic steel, and its correlation with the Portevin-Le Chatelier (PLC) banding, was elucidated using the in-situ synchrotron XRD measurement and digital image correlation (DIC) method during tensile test. The average dislocation velocity beyond the PLC band ranged from 10^{-2} to 10^{-1} nm/s, while reached to the order of 10° nm/s within the PLC band. In comparison, carbon diffusivity was significantly lower, allowing carbon atoms to diffuse only from 10^{-7} to10^{-9} nm in one second. The findings indicate that dislocations beyond the advancing PLC band were pinned by nearby carbon atoms, while dislocations within the PLC band became de-pinned from the carbons. Such localized pinning and de-pinning of dislocations occurred sequentially during deformation, appearing as the propagation of PLC bands in macroscopic scale.
58.	Monitoring post-mining reclamation success in Jharia Coalfield using geospatial technology **V Saini** - Journal of the Indian Society of Remote Sensing, 2024 **Abstract:** The widespread usage of coal for power generation necessitates continuing mining. While producing a valuable resource, this method significantly degrades the natural environment, notably the local vegetation. Once mining has stopped, reclaiming the destroyed areas to restore the natural landscape is critical. Mining activities have been going on for centuries; however, monitoring reclaimed areas through field-based methods is inefficient and time-consuming. In contrast, the expanding accessibility of geospatial data over the last five decades has aided in the accurate and consistent mapping and monitoring of reclaimed mining zones. Keeping in line, the present study utilized Landsat TM/OLI data from 2005 to 2021 to track reclamation success in a part of Jharia Coalfield, India. The methods included deriving Normalized Difference Vegetation Index (NDVI) images to evaluate the spatiotemporal variation of vegetation health, density, and vigour; and visual appreciation using a variety of RGB combinations of three date NDVI images. Later, a statistical threshold method based on Z-scores was employed to quantify the NDVI change values into three categories- Decrease, Unchanged and Increase. According to these analyses, the reclamation success in the study area ranged from modest to good. In the two focus areas, there has been an increase of 72 and 76 hectares in the Increase class. The accuracy of the classified change image was calculated to be 84.4 per cent. Until recently, no such work has been reported from the study area. The present research results are critical to mining professionals, environmentalists, and society and provide a promising way to inform about the success of

	reclamation activities and their monitoring.
59.	Numerical simulations of bio-inspired approaches to enhance underwater swimming efficiency **R Kumar, SS Padhee, D Samanta** - Physics of Fluids, 2024 **Abstract:** The present study discusses the numerical simulation results of swimming similar to manta rays. The complex three-dimensional kinematics of manta rays were implemented to unravel the intricacies of its propulsion mechanisms by using the discrete vortex method (DVM). The DVM replaces the requirement for a structured grid across the computational domain with a collection of vortex elements. This method simplifies grid generation, especially for intricate geometries, resulting in time and effort savings in meshing complex shapes. By modeling the pectoral fins with discrete panels and utilizing vortex rings to represent circulation and wake, the study accurately computes the pressure distribution, circulation distribution, lift coefficient, and thrust coefficient of the manta ray. This study focuses on the modulation of aerodynamic performance by altering the span length and the length change ratio during the downstroke and upstroke motion (SV). The manta ray's three-dimensional vortex configurations comprise a combination of vortex rings, vortex contrails, and horseshoe vortices. Analysis of the three-dimensional vortex structure indicates the presence of multiple vortex rings and horseshoe vortex rings at higher SV values, while adequate formation of horseshoe vortices is not observed at lower SV values. In terms of propulsive performance, both lift and thrust increase with SV, while the propulsive efficiency demonstrates its peak at $SV = 1.75$. The analysis reveals that at higher SV values, the net thrust generated primarily originates from the tip of the fins. Moreover, the study illustrates a significant enhancement in propulsive efficiency, particularly in association with optimal Strouhal numbers ranging between 0.3 and 0.4. The key findings of this study may be used in efficient design of agile autonomous underwater vehicles for marine exploration and surveillance applications.
60.	On designing a wavy sinusoidal micromixer for efficient mixing of viscoelastic fluids harnessing elastic instability and elastic turbulence phenomena **S Gupta**, **C Sasmal** - Chemical Engineering Science, 2024 **Abstract:** Effective mixing in microscale systems encounters difficulties due to the inherently low Reynolds numbers. This investigation delves into harnessing elastic instability and elastic turbulence phenomena to improve the mixing performance of viscoelastic fluids within a wavy sinusoidal micromixer with variable cross-sectional areas. Previous experiments demonstrated enhanced mixing efficiency, while our numerical simulations indicate that this enhancement is true up to a certain Weissenberg number. Beyond this threshold, a further increase in the Weissenberg number results in diminished mixing efficiency. Moreover, we observe that mixing efficiency increases with the Deborah number, albeit with an exponential increase in pressure drop. Conversely, mixing efficiency also increases with the number of turns in the micromixer, albeit with a linear increase in pressure drop. Hence, selecting a wavy micromixer with more turns and a relatively lower Deborah number is advisable for achieving comparable efficiency with reduced pressure drop. Additionally, the shear-thinning properties of viscoelastic fluids impede mixing efficiency by suppressing elastic instability and elastic turbulence phenomena. In conclusion, this study provides valuable insights for designing optimal wavy micromixers that effectively mix viscoelastic fluids by utilizing elastic instability and elastic turbulence phenomena.
61.	Pullout capacity analysis of horizontal plate anchors with tensile strength cutoff **R Ganesh** - International Journal of Geomechanics, 2024 **Abstract**: The conventional Mohr–Coulomb (M-C) failure criterion is commonly used in existing studies to determine the ultimate pullout capacity of plate anchors buried in cohesive-frictional soils. However, this criterion overestimates the tensile strength of these soils by

	assuming a linear failure envelope (in both compression and tensile regimes) within the normal-shear stress space. In this study, the ultimate pullout capacity of horizontally buried plate anchors in cohesive-frictional soils was determined, accounting for the effect of tensile strength cutoff. The study proposed a series of semianalytical solutions utilizing the kinematic horizontal slice approach and investigated the ultimate pullout capacity of four different anchor shapes, including circular, square, rectangular, and strip anchors. The impact of nonassociated flow rule on the results was also examined. It has been observed that the results obtained using the M-C failure criterion with a tension cutoff are significantly lower than those obtained using the conventional M-C failure criterion. The difference between both results increases as soil cohesive strength increases and anchor burial depth decreases. These findings clearly demonstrate that eliminating tensile strength from the strength envelope leads to a more conservative estimate of plate anchor pullout capacity. The study emphasizes changes in anchor failure surfaces for various parameter combinations and provides results that are consistent with specific solutions reported in the literature.
62.	Purely ionically bonded cation paving the way to ultralow thermal conductivity and large thermoelectric figure of merit in Ruddlesden-Popper Perovskite Cs2SnI2Br2 A Majumdar, S Chowdhury, **R Ahuja** - Journal of Physics: Condensed Matter, 2024 **Abstract:** Journal of Physics: Condensed Matter Purpose-led Publishing, find out more. ACCEPTED MANUSCRIPT Purely Ionically Bonded Cation Paving the Way to Ultralow Thermal Conductivity and Large Thermoelectric Figure of Merit in Ruddlesden-Popper Perovskite Cs2SnI2Br2 Arnab Majumdar1, Suman Chowdhury2 and Rajeev Ahuja3 Accepted Manuscript online 13 May 2024 • © 2024 IOP Publishing Ltd What is an Accepted Manuscript? DOI 10.1088/1361-648X/ad4aac DownloadAccepted Manuscript PDF Article metrics 44 Total downloads Submit Submit to this Journal Permissions Get permission to re-use this article Share this article Article and author information Abstract Lower dimensional materials have gained quite a bit of popularity in the last few decades. Perovskite materials have been studied extensively for their photovoltaic properties. But for large scale application of photovoltaic materials, the thermal properties need to be studied. In this work, using first principles calculations, we have studied the thermal conductivity and thermoelectric performance of quasi two-dimensional (2D) Ruddlesden-Popper phase of perovskite, Cs2SnI2Br2. The Cs atoms are found to be ionically bonded to the halogens leading to low elastic constants and hence give rise to weak bonding. The large anharmonicity in this material causes the lattice thermal conductivity to be ultralow having a value of 0.30 W.m-1.K-1 at 300 K and therefore the thermoelectric figure of merit has been found to be high with a maximum value of 2.08 at 600 K. This lead-free 2D perovskite can be the precursor to a wide variety of similar materials with ultralow thermal conductivity.
63.	Renewable aromatic hydrocarbons from waste cooking oil over hierarchical imidazole supported zeolites B Joshi, O Singh, A Agrawal…**N Gopinathan**… - Journal of Materials Chemistry A, 2024 **Abstract:** Unlike coal, oil, or natural gas, waste cooking oil (WCO) acts as a renewable source of carbon. It can be converted into energy, fuels, and fine chemicals, instead of being disposed of. This only requires appropriate logistics and a local supply chain network. In such a scenario, WCO can be viewed as a potential feedstock for the production of petrochemicals, particularly critical aromatic platform molecules for high-value chemicals. The study examined, the direct conversion of WCO into aromatic hydrocarbons on an imidazole-supported zeolite (ISZ) catalyst was investigated. The formation of aromatics was found to depend on the pore structure and acidity of the catalyst. The addition of metal oxides over ISZ enhances the Lewis acidic sites, which predominantly enhances the dehydrogenation reaction and yields more aromatic hydrocarbons. In addition, it was found that the average pore size of the catalyst is 6.3 nm, which effectively helps diffuse monoaromatics (C_6-C_8). To investigate the changes occurring on the

	catalyst surface during the reaction at different temperatures (25-500 °C), surface intermediates and products formed were closely monitored using in situ DRIFTS. Pyro-probe GC-MS study of the model compounds found in WCO showed that the cracking, cyclisation, and dehydrogenation pathway is responsible for the formation of aromatic hydrocarbons. The $Zn_{20}Cr_3$/ISZ showed excellent stability and good selectivity of C_6-C_8 aromatic species (65.9%) at 430 °C under atmospheric pressure and promise as a suitable catalyst candidate for high yield aromatics from WCO.
64.	Review of isomers in the A ≈ 135 region and nuclear shape evolution R Palit…**D Choudhury**, N Goel, **S Singh**… - The European Physical Journal Special Topics, 2024 **Abstract:** The measurements of lifetimes and electromagnetic moments of the isomeric states in some of the nuclei around 135 carried out at BARC-TIFR Pelletron Linac Facility at TIFR, Mumbai, are highlighted. The results from these measurements, along with similar studies reported in the literature, provide a wealth of nuclear structure information in Ba, La, and Ce isotopes in the 135 region. Comparison of the measured moments with the calculations gives a unique testing ground for the predictive power of the nuclear models. Plans for similar studies in other mass regions are also described at the end.
65.	Self-assembled dipeptide grafted nanohybrid material strips for reliable spectroscopic and electrochemical recognition of tryptamine Divya, S Saini, S Kalra, N Kaur, **N Singh** - Sensors and Actuators B: Chemical, 2024 **Abstract:** According to the World Health Organization (WHO), foods high in tryptamine may cause foodborne diseases and abnormal activity in the central nervous system (CNS). The real-time monitoring of tryptamine levels is an emphasized topic among scientific community. In the present work, we report a cost-effective fluorescent paper strips-based methodology impregnated with self-assembled dipeptide-modified (DM1) zinc oxide (ZnO) i.e. DM1@ZnO for the real-time monitoring of tryptamine levels. It is based on an organic-inorganic nanohybrid material of self-assembled N-functionalised dipeptide molecule coated over the surface of ZnO thus tailoring its properties for the detection of tryptamine employing spectroscopic and electrochemical methods. The designed material exhibited a noteworthy response towards tryptamine irrespective of the presence of other biogenic amines (BAs). It selectively displayed blue fluorescence under the 365 nm UV light. On top of that, the detection of tryptamine was also corroborated by its transition to 2-oxytryptamine, as deduced from its electrochemical route. Thus, the proposed paper strip-based methodology unbolts a realistic platform for the efficient recognition of varying levels of tryptamine thus tackling the prima facie reasons for foodborne diseases. 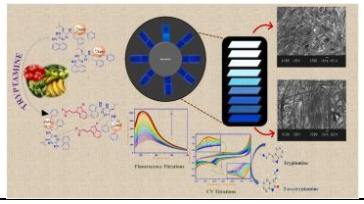
66.	Silver and copper nanoparticle-loaded self-assembled pseudo-peptide thiourea-based organic–inorganic hybrid gel with antibacterial and superhydrophobic properties for antifouling surfaces **R Devi, G Singh**, A Singh, J Singh, N Kaur, **N Singh** - ACS Applied Bio Materials, 2024 **Abstract:** The escalating threat of antimicrobial resistance has become a global health crisis. Therefore, there is a rising momentum in developing biomaterials with self-sanitizing capabilities and inherent antibacterial properties. Despite their promising antimicrobial properties, metal nanoparticles (MNPs) have several disadvantages, including increased toxicity as the particle size decreases, leading to oxidative stress and DNA damage that need consideration. One solution is

	surface functionalization with biocompatible organic ligands, which can improve nanoparticle dispersibility, reduce aggregation, and enable targeted delivery to microbial cells. The existing research predominantly concentrates on the advancement of peptide-based hydrogels for coating materials to prevent bacterial infection, with limited exploration of developing surface coatings using organogels. Herein, we have synthesized organogel-based coatings doped with MNPs that can offer superior hydrophobicity, oleophobicity, and high stability that are not easily achievable with hydrogels. The self-assembled gels displayed distinct morphologies, as revealed by scanning electron microscopy and atomic force microscopy. The cross-linked matrix helps in the controlled and sustained release of MNPs at the site of bacterial infection. The synthesized self-assembled gel@MNPs exhibited excellent antibacterial properties against harmful bacteria such as Escherichia coli and Staphylococcus aureus and reduced bacterial viability up to 95% within 4 h. Cytotoxicity testing against metazoan cells demonstrated that the gels doped with MNPs were nontoxic (IC50 > 100 μM) to mammalian cells. Furthermore, in this study, we coated the organogel@MNPs on cotton fabric and tested it against Gram +ve and Gram −ve bacteria. Additionally, the developed cotton fabric exhibited superhydrophobic properties and developed a barrier that limits the interaction between bacteria and the surface, making it difficult for bacteria to adhere and colonize, which holds potential as a valuable resource for self-cleaning coatings. 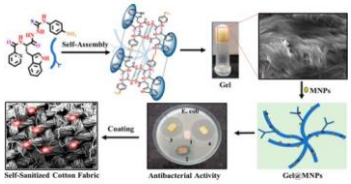
67.	Sulfonic acid functionalized SBA− 15 catalyst and mercaptopropionic acid promotor for the selective synthesis of p, p′− Bisphenol A: Replacement to mineral acid−based process **G Saini, AK Manal, R Srivastava** - Catalysis Today, 2024 **Abstract:** The significance of selective catalysis in producing plastic monomers is crucial to meet sustainability and economic requirements. It is essential to develop a selective solid acid catalyst to replace irrecoverable corrosive mineral acids and thermolabile sulfonated resins for the production of p,p′−bisphenol A (BPA) isomer, a key intermediate in polycarbonate production. However, limited success has been achieved due to low activity and selectivity towards the desired p,p′−BPA isomer. Herein, a mild and selective route is presented for producing p,p′−BPA using SBA-15 functionalized sulfonic acid catalysts. Sulfonic acid-based catalysts with and without alkyl chain linkers, supported on SBA−15, were synthesized to evaluate the effect of acidity, and textual properties on the catalytic efficiency, and product selectivity. Among all the synthesized catalysts, SBA−15−Pr−SO_3H exhibited the highest product selectivity. The addition of mercaptopropionic acid (as a promoter) enhanced the catalytic efficiency and afforded ∼99% acetone conversion, with 97.3% p,p′−BPA selectivity. A detailed mechanism with and without the promoter is proposed. The study also highlights the potential of mesoporous SBA−15−supported sulfonic acid catalysts as a selective and efficient catalyst for synthesizing bisphenol derivatives from the lignocellulose biomass−derived platform molecules, addressing challenges posed by fossil resources. 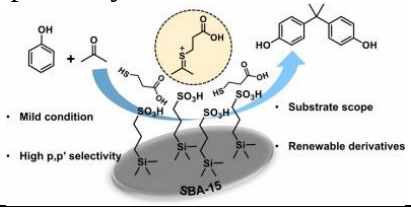
68.	Swell-shrink and microstructural response of expansive soil treated with nanomaterials **NJ Sahare, M Raheena** - International Journal of Geotechnical Engineering, 2024

	Abstract: Expansive soils like Black Cotton Soil, exhibit numerous engineering hurdles due to their high swell-shrink behaviour, resulting in structural instability. Traditional stabilization techniques often prove inadequate and available nanomaterials are expensive, creating a demand for a cost-effective and eco-friendly stabilizer like nano rice husk ash (nRHA). This study tackles the challenge of stabilizing expansive soil using nRHA, synthesized via two distinct ball milling methods. Various concentrations of nRHA (0%, 0.2%, 0.4%, 0.6%, 0.8%, and 1.0%) were tested to assess their effectiveness in reducing the swell-shrink behaviour of Black Cotton Soil.r Result indicate that a 0.4% dosage of 2 + 5 hours nRHA ($n_{2,0.4}$) significantly decreases the soil's swell-shrink potential. This treatment triggers the formation of Calcium Aluminium Oxide (CAO) and Calcium Aluminium Silicate Hydrate (CASH) gels, validated by X-ray diffraction (XRD) and Scanning electron microscope (SEM) analysis. This study advances nRHA treatments in enhancing the swell-shrink behaviour of expansive Soil.
69.	Tailoring the extension-bending-twisting coupling in composite laminates using carbon nanotube hybridization HS Bedi, **SS Padhee, P Agnihotri** - Modelling and Simulation in Materials Science and Engineering, 2024 **Abstract:** The existence of extension-bend-twist coupling of deformations in composites is a complex problem. Ability to tailor the coupling response as per the requirement is desirable to harness the high strength-to-weight ratio of composites in many structural applications. Here we report a feasible design strategy to tune the extent of deformation coupling in composite laminates. To this end, carbon nanotube (CNT) grafted lamina is incorporated in the lay-up of conventional composites. Classical laminate theory (CLT) and finite element analysis show that the coupling extent of extension-twist, extension-bending and extension- bending-twist can be suitably designed by varying the number, location and distribution of CNT grafted lamina in a laminate configuration. Theoretical and computational results reveal maximum extension-twist coupling when a single CNT grafted lamina is placed closer to the mid-plane in a 16 ply antisymmetric laminate. Symmetrical placement of CNT grafted lamina avoids the extension-bend coupling. Finite element analysis shows that the lateral bending of composite cantilever beam under combined axial and bending loads can be designed by suitably choosing the configuration of the modified laminate. These findings will significantly contribute in designing structural composites for advanced applications.
70.	Targeted information intervention among consumer clusters for electric vehicle penetration - A case study of Punjab, India **H Ahmad, TM Rahul** - Case Studies on Transport Policy, 2024 **Abstract:** Low success rates of existing EV adoption policies in India highlight the need for targeted policies to boost EV adoption. The current study employs a single-arm information intervention to analyse the impact of information provision on electric vehicle (EV) adoption among consumer clusters in a developing country context. Using Gaussian Mixed Modelling clustering, the sample was grouped into four segments based on three psychological latent variables. Clusters with greater pro-environmental values had higher pre-intervention positive purchase intention, signifying that policies aimed at promoting EVs among environmentally conscious consumers have higher chances of success. The intervention showed significant desirable changes in every cluster. Results indicate that such campaigns would achieve higher success in consumer clusters with low eco-friendliness. Appropriate measures for each cluster are suggested. The characteristics of consumer clusters with higher pre-intervention purchase intention could serve as guidelines for businesses and governments while formulating new and updating their existing EV policies.
71.	The blueprint of logical decisions in a NF-κB signaling system **P Gautam, SK Sinha** - ACS Omega, 2024

	Abstract: Nearly identical cells can exhibit substantially different responses to the same stimulus that causes phenotype diversity. Such interplay between phenotype diversity and the architecture of regulatory circuits is crucial since it determines the state of a biological cell. Here, we theoretically analyze how the circuit blueprints of NF-κB in cellular environments are formed and their role in determining the cells' metabolic state. The NF-κB is a collective name for a developmental conserved family of five different transcription factors that can form homodimers or heterodimers and often promote DNA looping to reprogram the inflammatory gene response. The NF-κB controls many biological functions, including cellular differentiation, proliferation, migration, and survival. Our model shows that nuclear localization of NF-κB differentially promotes logic operations such as AND, NAND, NOR, and OR in its regulatory network. Through the quantitative thermodynamic model of transcriptional regulation and systematic variation of promoter–enhancer interaction modes, we can account for the origin of various logic gates as formed in the NF-κB system. We further show that the interconversion or switching of logic gates yielded under systematic variations of the stimuli activity and DNA looping parameters. Such computation occurs in regulatory and signaling pathways in individual cells at a molecular scale, which one can exploit to design a biomolecular computer. 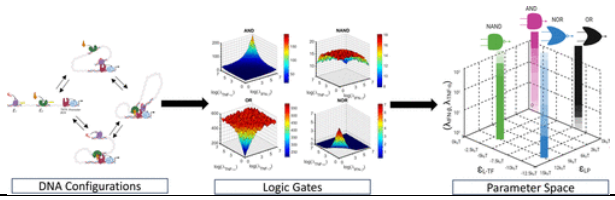
72.	The unit group of the group ring over $\mathbb{Z}n$ **H Setia, M Khan** - Communications in Algebra, 2024 **Abstract**: Let Zn be the ring of integers modulo n. Let Ct , Em , and Fr,s respectively denote the cyclic group of order t, the elementary abelian 2-group of order 2m , and the abelian group of exponent 4 with order 2r4s . In this article, we find the structure and generators of the unit group V(ZnC2). We also solve the normal complement problem in V(ZnC2) . Additionally, we provide a normal complement of Em in V(Z2nEm). At the end, we determine the structure of V(ZpnFr,s) for an odd prime p and establish that Fr,s does not have a normal complement in V(ZpnFr,s).
73.	Tribological performance in micro-milling of Ti6Al4V under nanofluid-based minimum quantity lubrication **J Airao**, A Jain, **CK Nirala**, D Ununе - International Journal on Interactive Design and Manufacturing (IJIDeM), 2024 **Abstract:** Micromachining processes, derived from scaled-down versions of conventional machining methods, have the potential to meet the growing demand for highly accurate and precise features in various parts. This work aims to explore the effect of distinct nanofluids on the micro-milling performance of Ti6Al4V, considering the size effect and tribological properties of different nanofluids developed indigenously. The cooling and lubrication approaches employed are minimum quantity lubrication (MQL) with Canola oil, nanoemulsion, and carbon nanotubes. Experiments are conducted at differing feed rates to account for the size effect resulting from cutting edge radius. Evaluation of tribological performance includes analysis of thermal conductivity and viscosity of each lubricant, tool wear, and surface morphology of machined slots. The results indicate that canola oil and nanoemulsion yield superior surface finishes at a low feed rate due to their lubricating properties, reducing friction and tool wear. In contrast, a dry environment lacks lubrication, leading to increased friction, tool wear, and a rougher surface finish. Results revealed a reduction in tool diameter by approximately 10–15% for dry conditions, 1–3% for Canola oil, and 3–4% with nanoemulsion. Thus, it can be concluded that MQL confers advantages in enhancing the tribological performance of cutting tools and

	workpieces during the micro-milling process, promoting sustainability. 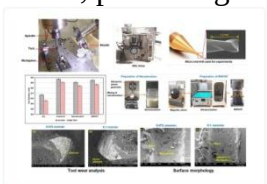
74.	UAV-enabled mobile RAN and RF-energy transfer protocol for enabling sustainable IoT in energy-constrained networks A Jaiswal, S Shivateja…**J Singh**… - IEEE Transactions on Green Communications and Networking, 2024 **Abstract:** his article introduces a novel approach for Unmanned Aerial Vehicles (UAV) assisted wireless power transfer (WPT) within a Radio Access Network (RAN) provisioned Internet of Things (IoT) network. The goal is to efficiently charge scattered IoT Nodes (INs) within their respective energy deadlines. The proposed methodology combines the concepts of Radio Frequency Energy Transfer (RFET) zones, K-means clustering, and Ant Colony Optimization (ACO) to optimize the charging process. Initially, RFET zones are formed around the INs, and K-means clustering is applied to group nodes based on their spatial proximity and energy requirements. Subsequently modified ACO algorithm is employed to construct efficient paths for UAVs to visit these clusters. This is achieved by taking into account several aspects such as node deadlines and UAV capacity, thereby assuring the timely and efficient transmission of energy.After comparative analysis with EUP-ACS and IA-DRL, the proposed algorithm achieves a substantial reduction of 22.22% and 36.36% respectively in UAV usage, while also exhibiting significant improvements in RFET zones, energy efficiency, and survival rate, confirming its effectiveness in enhancing charging performance, reducing energy waste, and meeting deadlines.
75.	Unleashing ultrahigh capacity and lasting stability: Aqueous zinc-sulfur batteries **S Mehta, S Kaur, M Singh, M Kumar, K Kumar, SK Meena, TC Nagaiah** - Advanced Energy Materials, 2024 **Abstract:** Despite of multifarious dominance of sulfur-based batteries, polysulfide-shuttling and use of high-cost organic electrolytes with flammability risks hinder their applicability as commercial devices. Herein a polysulfide-free aqueous zinc-sulfur (Zn─S) rechargeable battery is explored, which offers a low-cost and environmentally friendly energy storage system being Zn and Sulfur (S) highly abundant with high theoretical capacity. However, the stability of Zn anode is quite challenging due to dendritic growth and corrosion leading to the capacity decay. This work showcases the utilization of ethylene glycol (EG) and iodine (I2) as an electrolyte additive in aqueous zinc acetate [Zn(OAc)2] electrolyte for stabilizing the Zn─S battery performance. EG as an additive is able to mitigate the corrosion rate of the Zn electrode by 15 times which is supported by molecular dynamics simulation. The assembled Zn─S battery delivered an outstanding capacity of 1210 mA h g−1 at 0.1 C with a 91% capacity retention even after 250 cycles, along with remarkable reversible prolonged cycling stability of 3000 cycles at 1 C, with 64.5% capacity retention. More importantly, in situ electrochemical Raman spectroscopy is utilized to monitor the real-time formation of zinc sulfide (ZnS) as a single discharge product and simultaneously debunking the polysulfide shuttling in the system which is further supported by XPS, UV-Vis and IR spectroscopy.
76.	Visco-mechanical characterization of Molluscs (sea shell) biomimetics designs structures AI Ansari, NA Sheikh, **N Kumar** - Journal of the Brazilian Society of Mechanical Sciences and Engineering, 2024 **Abstract:** The study of biomimetics lattice structures, which frequently exhibit outstanding mechanical capabilities, is one of the hottest fields in modern new material/structural technology. The goal of this study is to analyze the nature optimize design of the Molluscs (Sea Shell) porous

	structure and bio-mimic the sea shell structure design for crashworthiness based on the structure's energy absorption nature and pore distribution. Initially, a micro-CT investigation was conducted to better understand the internal design structure and distribution of pores in the Costapex gastropod mollusks sea shell. Based on the examination of internal design structure and pattern, three different biomimetics designs, such as (a) shell with solid betel shape (SBS) structure, (b) shell with hollow betel shape (HBS) structure, (c) shell with concentrated hollow betel shape (CHBS) structure, were modeled on Abaqus simulia software and fabricated by additive manufacturing by utilizing ABS-M30i material. The computational and experiments compressive analysis at 0.5%, 1%, and 10% strain rate were conducted to study its mechanical properties, while digital image correlation (DIC) was performed simultaneously to study the strain field of the design structures. Furthermore, the dynamic mechanical analysis (DMA) was performed at 0.5% strain rate at different frequency to study the viscoelasticity nature of the design structure and the various outcomes of the simulation, experimental, DIC, and DMA analysis are summarizing in results section.

Disclaimer: This publication digest may not contain all the papers published. Library has compiled the publication data as per the alerts received from Scopus and Google Scholar for the affiliation "Indian Institute of Technology Ropar" for the month of May, 2024. The author(s) are requested to share their missing paper(s) details if any, for the inclusion in the next publication digest.